JOURNAL OF GEOPHYSICAL RESEARCH, VOL. 102, NO. A8, PAGES 17,611–17,624, AUGUST 1, 1997

Nonbouncing Pc 1 wave bursts

K. Mursula, R. Rasinkangas, and T. Bösinger

Department of Physical Sciences, University of Oulu, Oulu, Finland

R. E. Erlandson

Applied Physics Laboratory, Johns Hopkins University, Laurel, Maryland

P.-A. Lindqvist

Alfvén Laboratory, Royal Institute of Technology, Stockholm, Sweden

Abstract. On April 11, 1986, at about 0600 UT a long Pc 1 wave event of the hydromagnetic chorus type started on the ground, as registered by the Finnish pulsation magnetometer network. The main pulsation band at about 0.3 Hz was observed for several hours. Soon after start, this band smoothly extended to higher frequencies, forming another separate wave band which finally reached up to 0.5 Hz. During the event the Viking satellite was on its southbound pass over Scandinavia, close to the MLT sector of the ground network. From 0650 until 0657 UT, Viking observed a chain of Pc 1 bursts with increasing frequency. The strongest bursts could be grouped into two separate wave regions whose properties differed slightly. The higher-latitude region had a frequency of 0.3 Hz, well in agreement with the main Pc 1 band on the ground. The lower-latitude region contained the highest frequencies observed on the ground at about 0.5 Hz. The latitudinal extent of both wave regions was about 0.5°. They had slightly different normalized frequencies, Alfvén velocities, and repetition periods. Most interestingly, the repetition periods of both wave sources were too short for the bursts to be due to a wave packet bouncing between the two hemispheres. The results give new information about the high-latitude Pc 1 waves, showing that they can consist of separate repetitive but nonbouncing bursts. We suggest that the long-held bouncing wave packet hypothesis is generally incorrect and discuss two alternative models where the burst structure is formed at the equatorial source region of the waves.

1. Introduction

Energetic ions with temperature anisotropy are subject to the ion cyclotron instability and give rise to electromagnetic ion cyclotron (EMIC) waves [*Brice*, 1965; *Cornwall*, 1965, 1966; *Kennel and Petschek*, 1966]. These waves can, in favorable conditions, propagate to the ground and be observed as Pc 1 pulsations [*McPherron et al.*, 1972; *Bossen et al.*, 1976]. After their first observation in 1936 [*Sucksdorff*, 1936; *Harang*, 1936] the Pc 1 waves have been studied extensively on the ground (for early reviews, see, e.g., *Troitskaya and Guglielmi* [1967] and *Saito* [1969]) and later in situ by space observations, using low-altitude [e.g., *Iyemori and Hayashi*, 1989; *Mursula et al.*, 1994a; *Erlandson and Anderson*, 1996], midaltitude [e.g., *Taylor and Lyons*, 1976; *Erlandson et al.*, 1990, 1992], geostationary [*McPherron et al.*, 1972; *Bossen et al.*, 1976; *Roux et al.*, 1982], and high-altitude satellites [*Kaye and Kivelson*, 1979; *Anderson et al.*, 1992a, b; *Fraser et al.*, 1996].

The different types of Pc 1 waves observed on the ground have been classified according to their morphological appearance in sonagrams (dynamic spectra) [*Fukunishi et al.*, 1981]. At low latitudes and midlatitudes the most common Pc 1 type is the pearl pulsation [*Benioff*, 1960], also called structured Pc 1, which consists of clearly separate and regularly repeated wave bursts or pearls. The generally accepted model of pearl pulsations, which was already presented more than 30 years ago [*Jacobs and Watanabe*, 1964; *Obayashi*, 1965], assumes that the pearls are due to a wave packet, propagating along the magnetic field line and bouncing from one hemisphere to another, with subsequent losses at the two conjugate points being compensated by wave growth at the equator [*Criswell*, 1969; *Gendrin et al.*, 1971]. Different methods using ground-based [*Roth and Orr*, 1975; *Lewis et al.*, 1977; *Webster and Fraser*, 1985] and satellite observations [*Taylor and Lyons*, 1976; *Fraser et al.*, 1989; *Erlandson et al.*, 1990,

Paper number 97JA01080.
0148-0227/97/97JA-01080$09.00

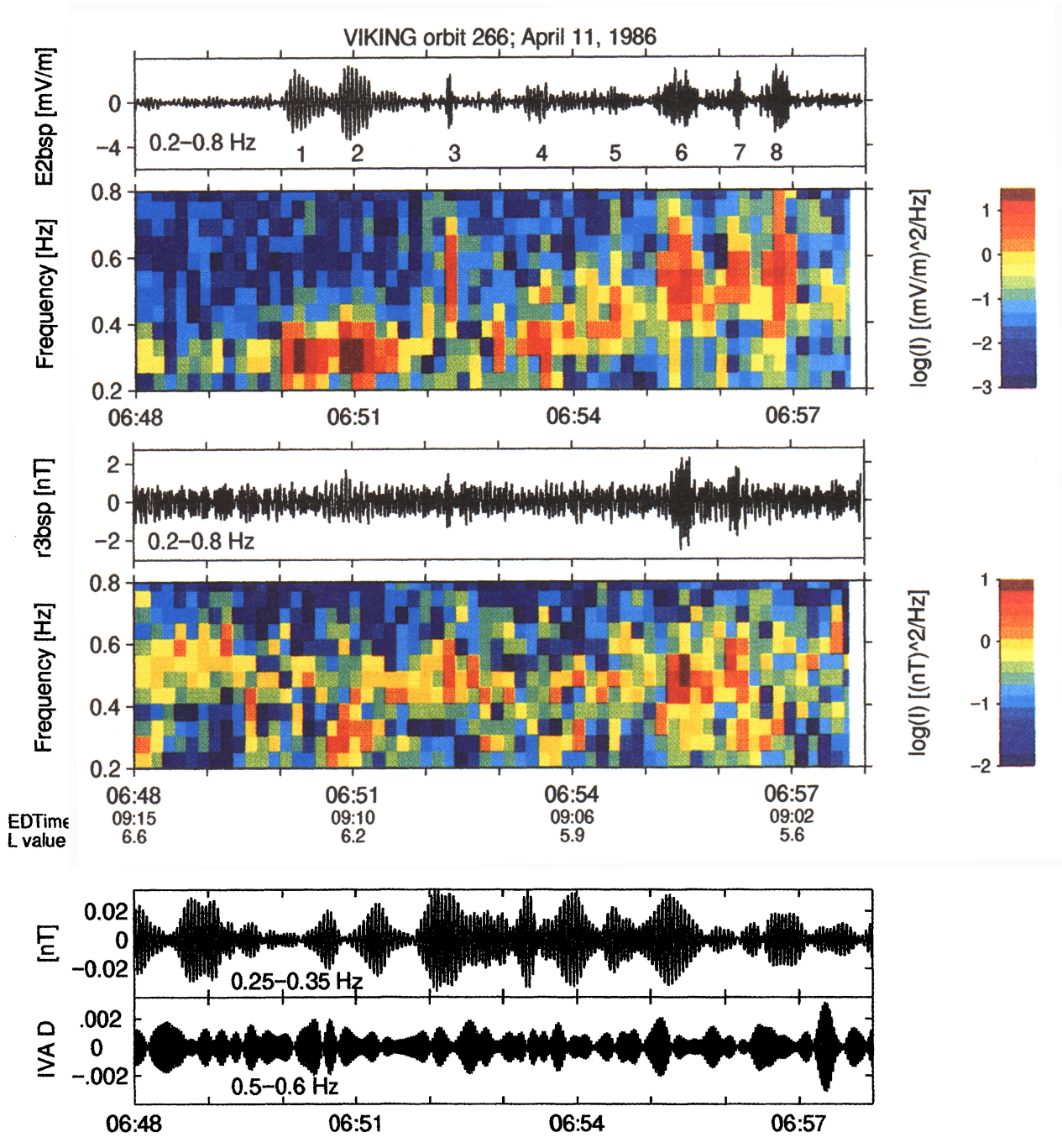

Plate 1. Waveform (band-pass filtered for 0.2-0.8 Hz) and dynamic spectrum for (top) the electric field $E2$ component (transverse to the magnetic field in spin plane) and (middle) for the magnetic field $r3$ component (along spin axis, almost transverse to magnetic field). Waveform of D component at IVA station (bottom) filtered in two frequency ranges (0.25-0.35 Hz and 0.5-0.6 Hz).

1992, 1996] locate the pearl Pc 1's mainly inside but close to the plasmapause where, because of the guidance of waves by plasma gradients, appropriate conditions for wave propagation and growth are expected [*Mazur and Potapov,* 1983; *Thorne and Horne,* 1992].

However, Pc 1 wave types other than pearl pulsations dominate the ground-based observations at high latitudes above approximately $L = 5$ [*Fukunishi et al.,* 1981; *Mursula et al.,* 1994b]. Also, satellite studies show that very few structured Pc 1 waves are observed at and beyond the geostationary orbit [*Gendrin et al.,* 1978]. Since the high-latitude Pc 1's are not as clearly structured as the pearl pulsations, they are sometimes generically called unstructured pulsations. Note, however, that occasional pearls or other bursts of varying intensity can appear among a more diffuse background even in these Pc 1 types. This is true in particular for a common high-latitude Pc 1 wave type called the hydromagnetic (HM) chorus [*Fukunishi et al.,* 1981]. Satellite observations show [*Bossen et al.,* 1976; *Anderson et*

al., 1992a] that EMIC wave occurrence at the equator maximizes in the postnoon sector, with increasing probability of wave occurrence for increasing equatorial distance at least up to about $L = 8$. This is in agreement with ground observations where maximum occurrence of (mainly unstructured) Pc 1's is found at auroral latitudes [*Troitskaya and Guglielmi*, 1970]. Moreover, the diurnal MLT distribution of unstructured Pc 1 waves on the ground coincides with that of equatorial EMIC waves [*Mursula et al.*, 1996]. Accordingly, the spatial distributions of structured and unstructured pulsations are rather different. The former prefer the plasmasphere, and the latter prefer the plasmatrough (plasma sheet) region.

The repetition period of pearls on the ground is typically a couple of minutes. Ground-based Pc 1 pearl observations depict a fair correlation between the pearl repetition rate T and wave period t [see, e.g., *Troitskaya and Guglielmi*, 1967] with a proportionality constant of about 100 (when the times are given in seconds). The pearl repetition period has also been estimated from a number of satellite studies where repeated Pc 1 bursts were observed. For example, *Fraser et al.* [1989] observed repetition periods from 135 s to 160 s for a structured Pc 1 wave at frequency f = 0.65 Hz and source region at $L = 4.7$. *Erlandson et al.* [1996] obtained a repetition rate of 154 s at f = 0.6 Hz and $L = 5.3$. Somewhat shorter repetition periods (T = 55-60 s) and higher frequencies (f = 1.5 Hz) were observed by *Erlandson et al.* [1992] at lower latitudes ($L = 4$). In all these cases the above relation between the two periods holds reasonably well. In spite of this success the results do not prove the bouncing wave packet (BWP) hypothesis but only verify the experimental consistency between satellite and ground wave observations. In order to have strong support for the BWP model the observed repetition periods should be the same as those calculated theoretically. However, the theoretical estimates are greatly dependent on various plasma parameters, in particular, the amount and distribution of equatorial heavy ions which strongly affect the wave group velocity when the wave frequency is close to a heavy ion gyrofrequency [*Fraser*, 1972; *Ludlow and Hughes*, 1993]. *Erlandson et al.* [1992] calculated that, for example, a change in latitudinal width of equatorial cold helium ions from 1° to 10° increased the repetition time by a factor of 2. Furthermore, *Ludlow and Hughes* [1993] showed that the temperature (warm plasma) effects can significantly change the repetition period compared to the cold plasma estimate. Therefore the theoretical calculations cannot give a sufficiently accurate estimate in order to give firm evidence for the BWP hypothesis.

Several studies have investigated the direction of propagation of waves in the magnetosphere. A common method has been to calculate the wave Poynting flux. This has been used for near-equatorial [*Mauk and McPherron*, 1980; *LaBelle and Treumann*, 1992; *Fraser et al.*, 1996] as well as midaltitude [*Erlandson et al.*, 1990] observations with the result that most flux is directed away from the equator into the ionosphere. The same result was obtained by *Erlandson et al.* [1996] using the lag of the cross-correlation function of waves observed in space at midaltitudes and ground. Furthermore, *Erlandson et al.* [1990] found that the waves at midaltitudes were propagating nearly in the direction of the background magnetic field, suggesting that the wave source was at a higher altitude along the field line. In the bouncing wave packet hypothesis the observation of downward propagating Pc 1 waves is reconciled by arguing that while the wave energy is mainly directed into the ionosphere, a sufficiently large fraction of waves are reflected back toward the equator. However, *Erlandson et al.* [1992] found that especially during the most intense Pc 1 pearl waves the amount of reflected wave power was quite small, less than about 10-20%.

In this paper we present the firsts results of a detailed analysis of a HM chorus type Pc 1 wave event observed in the magnetosphere at midaltitudes by the Swedish Viking satellite and on the ground by the Finnish search-coil magnetometers at Kilpisjärvi (KIL), Ivalo (IVA), and Rovaniemi (ROV) (see Table 1 for coordinates of the stations). The event started on April 11, 1986, at about 0600 UT, and Pc 1 wave activity lasted as a nearly continuous band on the ground until about 1400 UT. Roughly 1 hour after the start of the event the Viking satellite was on its southbound pass (orbit 266) over Scandinavia at the altitude of about 13000 km in the late morning sector at 09 MLT. The ionospheric footpoint of the satellite was close to the Finnish network. (See Figure 1 for Viking footpoint location. For a review of the Viking satellite, see *Hultqvist* [1987].) In the next section we will present the wave observations at Viking and on the ground. In section 3 we will discuss the large-scale evolution of the event, which led to the Viking observation of two separate and different Pc 1 wave source regions. Several detailed properties of these sources (e.g., normalized frequencies, amplitudes, Alfvén velocities, latitudinal widths, and repetition periods) are derived from Viking observations. Both wave regions consist of separate bursts repeated at a fairly short and nearly equal repetition period. We will argue that the bursts cannot be due to a bouncing wave packet and discuss some alternatives to the BWP hypothesis. Finally, section 4 presents our summary and conclusions.

2. Observations

2.1. Viking Observations

From 0650 until 0657 UT several bursts of Pc 1 activity were seen in both electric and magnetic field measurements. Plate 1 depicts the waveform (filtered in view of better visibility for relevant frequencies from 0.2 to 0.8 Hz) and the dynamic spectra for one electric component ($E2$, perpendicular to the ambient magnetic field) and one magnetic component ($r3$, perpen-

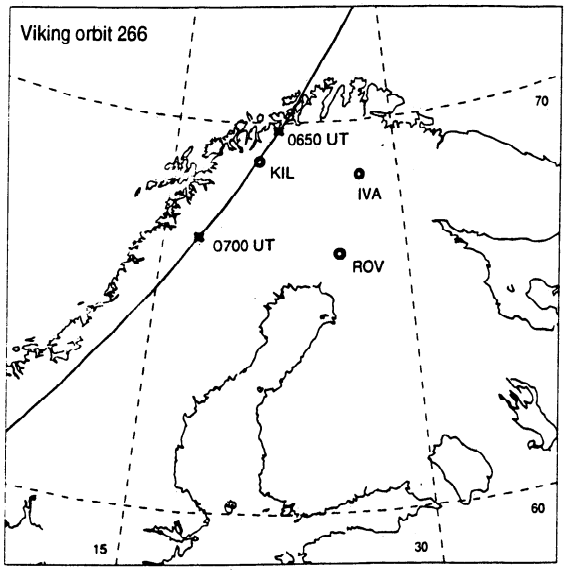

Figure 1. The track of the ionospheric footpoint of the Viking satellite over Fenno-Scandia during the event. The Viking wave observations were constrained between the two times marked in the figure by crosses. The three Finnish stations Kilpisjärvi (KIL), Ivalo (IVA), and Rovaniemi (ROV) are marked by circles. Latitudes and longitudes are geographic.

dicular to electric field and almost perpendicular to ambient magnetic field; magnetic components are residuals where a model value has been extracted from the observed field). Viking was in a cartwheel spinning mode, measuring two components of electric field in the spin plane, one mainly field-aligned, the other perpendicular to the ambient magnetic field. During the time of Pc 1 wave observations, Viking was headed equatorward, crossing invariant latitudes from $L = 6.3$ to $L = 5.6$ at about 09 MLT.

The eight separate wave bursts (B1-B8) observed by the electric field were numbered in order of detection in Plate 1. The largest five bursts among these are grouped in two separate wave regions: the first one at about 0650-0651 UT consisting of B1 and B2 with a low wave frequency of about 0.3 Hz, and the second one consisting of B6, B7, and B8 at about 0655-0657 UT with a higher wave frequency of about 0.5 Hz. We will thus call the first region the low-frequency wave source and the second region the high-frequency source. Between these two regions of large amplitude bursts a few weaker wave bursts are observed. Of these, B3 has a fairly high amplitude but a very short duration. It has a similar frequency as waves of the high-frequency source, which appear slightly later. Bursts 4 and 5 are rather weak. The frequency of B4 is slightly above that of the low-frequency source, and B5 has a frequency of about 0.4 Hz, clearly between the frequencies of the two main sources. Accordingly, there is indication of a weak third source of Pc 1 waves, which we will call the intermediate-frequency source. Note that neglecting B3, the frequency of wave bursts observed by Viking increases continuously as the spacecraft flies from high to low latitudes.

Some wave bursts are less clearly observed in the magnetic field than in the electric field (see Plate 1). This is mainly due to the relatively lower sensitivity of the magnetic field sensor for detecting waves of such a small amplitude from the fairly large background magnetic field at Viking altitude. (The viability of the Viking magnetic field instrument to observe EMIC waves was earlier demonstrated by *Erlandson et al.*, [1990].) Accordingly, the magnetic field amplitudes of the bursts in Plate 1 are rather low in comparison to background noise. Nevertheless, bursts 2, 3, 6, and 7 are strong enough to stand out even in the waveform of the magnetic $r3$ component. Furthermore, the magnetic field spectrogram (Plate 1) shows a quite similar overall pattern as the electric field and verifies that these four bursts have the same frequencies in the magnetic and electric fields. (The same results were obtained for the other perpendicular magnetic component ($r2$), where some of the bursts, e.g., B2 and B8, are seen even more clearly than in $r3$. However, since the corresponding electric component ($E3$) is not available, we do not use the $r2$ component in the paper.) Therefore the magnetic field amplitudes of these bursts are large enough to be considered reliable measurements of the magnetic component of corresponding Pc 1 waves. Finally, we already note that (see Plate 1) the largest electric amplitudes are found for the low-frequency source, but the largest magnetic field amplitudes are found for the high-frequency source. A more accurate analysis of this and other differences between the two main wave sources is postponed to section 3.

2.2. Ground-Based Observations

Plate 1 also includes the waveform of the D component observed at the IVA station simultaneously at the time of the Viking Pc 1 wave bursts. The IVA waveform was band-pass filtered in two frequency ranges (0.25-0.35 Hz and 0.5-0.6 Hz) around the frequencies of the two Viking wave sources so as to increase the correspondence between ground and Viking for bursts from the two sources. Plate 1 shows that the ground signal was modulated at roughly the same period as observed by Viking. (This is more clear for the stronger low-frequency signal). In a detailed comparison, for example, the two Viking low-frequency bursts match well with the two bursts observed at IVA some 15-20 s later. The higher-frequency signal is much weaker and therefore more noisy, but even there, during the Viking high-frequency bursts a sequence of bursts is observed with repetition period and time delay in reasonable agreement with Viking observations. The overall time delay of ground bursts corresponds well with the expected time delay for waves propagating from Viking to ground. Such a correlation between Viking and ground bursts verifies, for example, that the bursts observed by Viking are temporal rather than spatial.

In a larger timescale, Figure 2 depicts the dynamic spectra at three Finnish stations in an isocontour line presentation from the start of the event prior to 0600 UT until after 0900 UT. As seen in Figure 2, the three ground stations observe a nearly continuous band of waves with maximum power at about 0.3 Hz for most of the nearly 4 hour time interval depicted. This frequency range corresponds well to the low-frequency wave source observed by Viking. We have studied this question in more detail by calculating power spectra for the three ground stations and the Viking electric field at specific time intervals. Figure 3a and 3b depict power spectra at the time when Viking observed the low-frequency and high-frequency wave source, respectively, and Figure 3c corresponds to a later time after the Viking flyby. Figure 3a shows that all three ground stations have a power maximum at about 0.3 Hz, in good agreement with the frequency of the simultaneous Viking low-frequency source. Note also that during the observation of the low-frequency waves, Viking was at a slightly higher invariant latitude than KIL, the highest-latitude station of the chain. Figure 3a shows that the wave power of the 0.3 Hz maximum decreases with decreasing latitude of the station, with KIL having the largest power and ROV having the smallest. This also suggests that the low-frequency source was closest to the L shell of the KIL station.

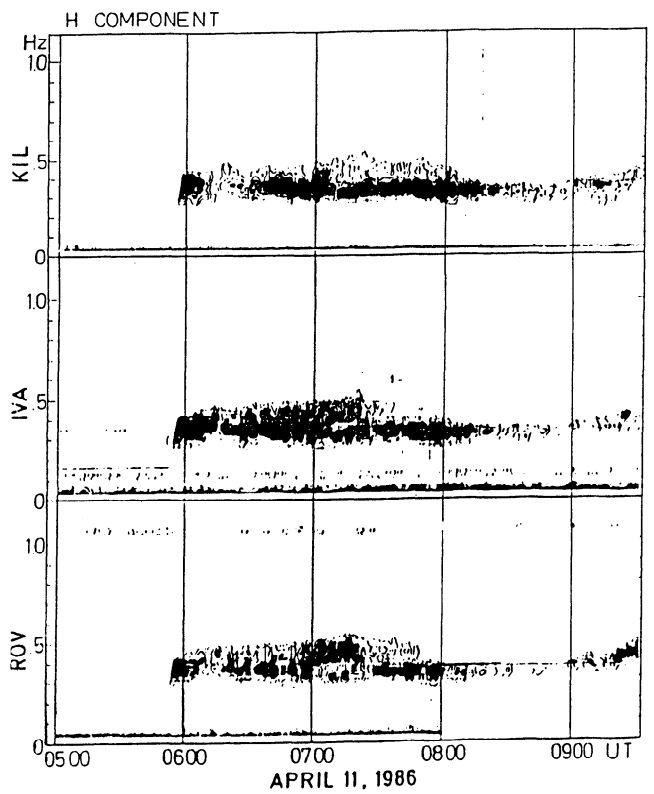

Figure 2. The dynamic spectra of the H component registered at KIL, IVA, and ROV showing Pc 1 waves with frequency between 0.3 Hz and 0.5 Hz. The amplitude is given as isocontour lines with 6 dB per step. (The narrow weak line in the ROV spectrum just above 1 Hz is due to a perturbation.)

The low-frequency source is seen as a corresponding maximum in the ground station power spectra even at later times, for example during the Viking high-frequency wave observations (Figure 3b) and after the Viking flyby (Figure 3c). Note that the power of the low-frequency source at KIL stays almost invariant for the times plotted in Figure 3, demonstrating the great stability and persistence of the low-frequency source. The low-frequency power at the two lower-latitude stations (IVA and ROV) varies somewhat more but remains the same within a factor of 2 between Figure 3a and 3c. (At the time of Figure 3b the low-frequency source is divided into two peaks, which excludes straightforward comparison.)

Figure 3 shows that the Viking intermediate-frequency source at about 0.4 Hz is also observed on the ground. This wave source is seen as a separate maximum at about 0.4 Hz in the power spectra of the two lower-latitude stations at all the times plotted in Figure 3. The intermediate-frequency source is weakly seen even at KIL, either as a small spectral peak (Figure 3a and 3c) or as a spectral knee (Figure 3b). In particular, during the Viking flyby (Figure 3a and 3b) the power of intermediate-frequency waves is clearly strongest at the IVA station. Furthermore, Figure 3b shows that the power of the intermediate peak at IVA greatly exceeds that of the low-frequency source. These facts imply that the intermediate-frequency source is, at this time, located at a lower latitude than the low-frequency source, closest to the L shell of IVA station. Overall, the power of the intermediate-frequency source at the lower-latitude stations varies roughly by a factor of 4-5.

It is also interesting to note that the Viking high-frequency (0.5 Hz) wave source is only observed as a simultaneous spectral knee at the three ground stations (Figure 3b). (A similar knee is observed on the ground in Figure 3a prior to the Viking observation of this source.) However, there is clear evidence that the spectral power of the Viking high-frequency source is increasing with time at all three stations. This is particularly visible after the Viking flyby in Figure 3c, where the related power is enhanced by a factor of 3-5 with respect to Figure 3a and 3b and the spectral knees in Figure 3a and 3b have turned to small spectral peaks at 0.5 Hz in Figure 3c. This development is also seen in the dynamic spectra of Figure 2 as a continuous extension of the spectrum toward higher frequencies during the event. (This will be discussed more in the next section.)

We have also included in Figure 3 the values of the equatorial helium gyrofrequencies calculated for each station corresponding to the conditions during the event (see also Table 1). The gyrofrequencies of IVA and ROV stations are clearly but not very far above the 0.3-0.5 Hz frequency range, where main wave power is observed. Note that a sharp dropout in wave power is observed at all stations close to the KIL gyrofrequency in Figure 3a. As higher frequencies are further enhanced later in time

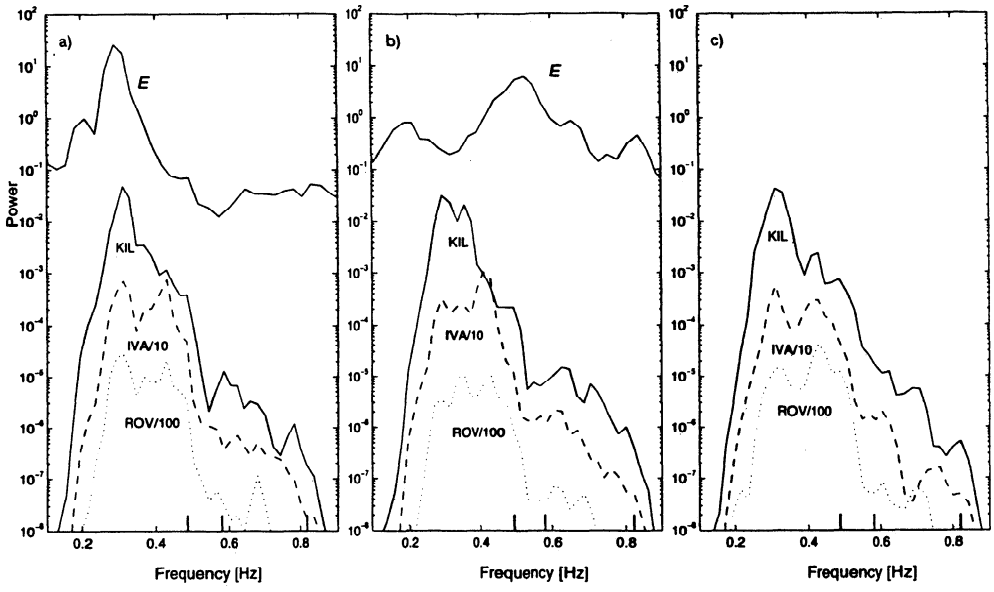

Figure 3. Power spectra of Viking E field (upper solid line) and the H component of three ground stations KIL (lower solid line), IVA (dashed), and ROV (dotted) for (a) 0650-0652 UT, (b) 0655-0657 UT, and (c) 0716-0718 UT. The power of the IVA (ROV) station has been scaled down by 10 (100) with respect to KIL. The equatorial He^+ gyrofrequencies of the stations (given in Table 1) are noted in each plot as vertical ticks on the x axis.

(Figure 3b and 3c), this dropout becomes more diffuse and moves to a slightly higher frequency between the KIL and IVA gyrofrequencies.

3. Discussion

3.1. Large-Scale Evolution of Wave Sources

The period of observations studied in this paper was very quiet geomagnetically, and Kp was 1+ during the 3 hour interval from 0600 to 0900 UT. Dst was about -25 nT after a minor storm (minimum -50 nT) that occurred during the previous day. This indicates that a considerable amount of energetic ions existed in the ring current during the observations. Furthermore, a considerable substorm with an AE index reaching nearly 500 nT occurred at 0400-0500 UT. This caused a small decrease in Dst at 0500 UT, indicating a new enhancement of the ring current by substorm particles. The Pc 1 wave activity studied here started soon after this additional ring current enhancement.

As mentioned above, the energy for EMIC waves is supplied by energetic ions with temperature anisotropy ($T_\perp > T_\parallel$) [*Brice*, 1965; *Cornwall*, 1965, 1966; *Kennel and Petschek*, 1966; *Mauk and McPherron*, 1980; *Young et al.*, 1981]. The ions are also drifting around the Earth on some range of L shells. The main drift shell of ions producing the low-frequency EMIC waves was, at least over this 2 hour MLT range in the late morning sector, at about $L = 6.1$-6.3, as determined by Viking (see Plate 1). As seen above (Figures 2 and 3), the low-frequency wave source was quite stable, attaining a comparable high power for more than 2 hours. Given the above mentioned connection between waves and ions, the stability and persistency of low-frequency waves on the ground must reflect the similar stability of source ions. Low geomagnetic activity during the event suggests that no major changes occurred in the magnetospheric structure. Accordingly, ion drift conditions remained fairly stable, leading to a smooth evolution of wave activity on the ground.

In addition to the low-frequency band at 0.3 Hz, there were waves even at higher frequencies. As depicted in Figure 2, waves above the low-frequency band appeared soon after the start of wave activity on the ground, and

Table 1. Data of Three Finnish Search-Coil Magnetometer Stations

	Geographic		Corrected Geomagnetic		L	MLT at	Equatorial
Station	Latitude	Longitude	Latitude	Longitude	Value	0650 UT	$f_g(He^+)$, Hz
Kilpisjarvi	69.0	20.9	65.9	105.3	6.0	0904	0.49
Ivalo	68.7	27.3	65.0	109.8	5.6	0923	0.58
Rovaniemi	66.8	25.9	63.4	107.3	4.7	0913	0.82

Here $f_g(He^+)$, equatorial He^+ gyrofrequency.

by 0620 UT they already formed a separate spectral maximum, i.e., a separate wave band. This second band was continuously and smoothly extending to higher frequencies during the whole time of its existence until a decrease in intensity after 0720 UT. This band includes the intermediate-frequency (0.4 Hz) waves observed, for example, during the Viking flyby (Figures 3a and 3b) and the high-frequency (0.5 Hz) waves slightly later. The existence of this second band and its continuous extension to higher frequencies can be understood by a radially inward spreading or diffusion of energetic ions to lower L shells with a higher magnetic intensity and ion gyrofrequency. The common origin of the two wave bands and their smooth separation suggests that the ions producing the second band are originally part of the ion population responsible for the low-frequency band. When moving to lower L shells, increasing plasma density can lower the critical ion energy [*Gendrin et al.*, 1971] and thus enhance wave growth at the leading edge of the spreading ion cloud. This can explain why Viking observes two separate wave bands with minor wave activity in between, rather than one band with a large frequency spread and equally distributed wave power.

The second band and its development is most clearly seen at the IVA station, where its intensity was roughly equal to the intensity of the low-frequency band for a long time (see Figures 2 and 3). In particular, during the Viking flyby (Figures 3a and 3b) the power of the second band was clearly higher at IVA than at KIL or ROV. This verifies that by this time the source region of the second band was located equatorward of the low-frequency band, closest to the IVA station. Somewhat later, soon after 0700 UT the second band attains its highest power at ROV (see Figures 2 and 3c). This development gives further evidence that the source region of the second band was really moving to lower latitudes during the event.

3.2. Frequencies of Viking Wave Bursts

As already mentioned (see also Plate 1), the frequency of all Viking wave bursts except for B3 increased with decreasing latitude of the satellite. This is, of course, expected because of the higher value of the equatorial magnetic field and the higher equatorial ion gyrofrequency at lower latitudes. We have tabulated in Table 2 some properties of four of the main Viking bursts (B2, B3, B6, and B7). The frequencies (denoted by f) of all bursts are below the calculated equatorial helium gyrofrequency $f_g(\mathrm{He}^+)$ [*Tsyganenko*, 1989]. This frequency range corresponds well to the wave growth region between oxygen and helium gyrofrequencies, which is favored when a nonnegligible amount of He^+ ions exists [*Kozyra et al.*, 1984, and references therein]. On the basis of earlier Viking Pc 1 wave observations, *Erlandson et al.* [1990] found that in the L value range from $L = 4.5$ to about $L = 8$ (including the present case), waves were generated both above and below the corresponding equatorial helium gyrofrequency. However, at higher (lower) L the waves were found dominantly above (below) the helium gyrofrequency. *Gomberoff and Neira* [1983] noted that in the case of a large temperature anisotropy the waves are preferably produced above the helium gyrofrequency. This suggests a moderate anisotropy of about $A \simeq 1$ in the present case. *Horne and Thorne* [1994] calculated the wave growth in the outer magnetosphere and found great differences in the unstable frequency for different density conditions at different MLT sectors. Our observation in the prenoon sector agrees with their result of enhanced wave growth below $f_g(\mathrm{He}^+)$ at dayside.

Note also that the frequency of the bursts increased somewhat faster with decreasing latitude than with the calculated He^+ gyrofrequency, thus leading to the observation that the normalized frequency $f/f_g(\mathrm{He}^+)$ of the low-frequency source was slightly lower (about 0.6) than that of the high-frequency source (about 0.8). Of course, this result suffers from problems related to field line mapping and is based on small statistics. However, taken at face value, this observation may sound somewhat surprising, and it is interesting to study possible causes of the difference. Therefore we calculated the wave growth rate for reasonable plasma parameter values (at the equator where EMIC waves are generated) and its variation as a function of invariant lati-

Table 2. Properties for Four Viking Pc 1 Wave Bursts

	B2	B3	B6	B7
UT	0651:00	0652:20	0655:30	0656:10
L	6.2	6.1	5.8	5.7
f, Hz	0.28	0.49	0.46	0.51
$f_g(\mathrm{He}^+)$, Hz	0.46	0.50	0.58	0.59
$f/f_g(\mathrm{He}^+)$	0.61	0.98	0.79	0.86
$A(E2)pp$, mV/m	6.8	5.1	5.0	5.3
$A(B3)pp$, nT	2.4	3.1	4.6	4.1
V_A, km/s	2800	1600	1100	1300

Here f, wave frequency; f_g, equatorial He^+ gyrofrequency; f/f_g, frequency ratio; $A(E2)$, electric field amplitude; $A(B3)$, magnetic field amplitude; V_A, Alfvén speed.

tude, while keeping the plasma parameters fixed. (A change in L value leads to a corresponding change in magnetic field intensity in the dipole model.) For example, for a mixture of cold plasma (90% protons, 10% helium, density 50 cm^{-3}) and warm ions (99% protons, 1% helium, density 1 cm^{-3}, perpendicular temperature 50 keV, anisotropy $A = 1$) we found that the normalized frequency attains the value of 0.6 at about $L = 6$, which agrees very well with the observed normalized frequency of the low-frequency waves. Even more interestingly, the normalized frequency increases with decreasing invariant latitude and, for the above-mentioned parameter values, explains about half of the observed increase in normalized frequency between the two main wave regions. Moreover, the same qualitative behavior was observed for a large range of reasonable parameter values, not only for those mentioned above. Accordingly, the observed increase in normalized frequency is indeed expected and can be understood without sizable changes in plasma environment between the two main wave regions.

As an additional exercise, we also studied the variation of the normalized frequency as a function of some equatorial plasma parameters. For example, there is hardly any change in normalized frequency when the density of energetic ions is varied in a reasonable range of values (but keeping other plasma parameters and L shell fixed). However, increasing equatorial cold plasma density will decrease the normalized frequency, but the change is very slow. In order to counteract the above mentioned increase of normalized frequency with decreasing latitude, equatorial plasma density of the high-frequency waves should be about 10 times larger than that of the low-frequency waves. Given the short distance between the two wave regions, such a large change is not expected.

More interestingly, we found that the normalized frequency increases when the perpendicular temperature of the energetic ions decreases. A change of temperature from 50 keV to about 20 keV can alone explain the observed increase of the normalized frequency from 0.6 to 0.8. Taking the decrease of the L shell into account, even a smaller decrease in temperature is sufficient to explain the whole change. Therefore the observed increase in normalized frequency suggests that the energetic ions have indeed lost some energy into waves before reaching the lower latitudes of the high-frequency wave region. Note that the same mechanism, i.e., a gradual loss of ion energy during the event, can also explain the finite duration of the high-frequency wave band. This mechanism would imply that the amplitude of the second band decreases unless other factors compensate the effect. However, while moving to lower latitudes, the increasing cold plasma density could act as such a compensating factor, since wave growth increases with increasing plasma density [*Cornwall,* 1965; *Gendrin et al.,* 1971]. Therefore the second band may have a considerable power for some time even at quite low latitudes, in agreement, for example, with the large power of the ROV station in Figure 3c. This is also in agreement with the above mentioned view that waves are enhanced at the equatorward edge of the expanding ion cloud, leading to two distinct wave bands with only minor activity between these two regions.

3.3. Amplitudes and Alfvén Velocities of Viking Wave Bursts

Table 2 also depicts the electric and magnetic field amplitudes of the four Viking wave bursts. As already noted above, the Viking electric and magnetic fields seem to vary differently, the former slightly decreasing and the latter sizably increasing with decreasing latitude. Accordingly, the electric $E2$ component of the low-frequency waves (e.g., B2) is somewhat larger than that of the high-frequency waves (e.g., B6 and B7), while the reverse is true for the corresponding magnetic $r3$ component. We have calculated the ratio of these orthogonal electric and magnetic components in order to obtain a rough estimate for the local Alfvén velocity. (Actually, this estimate requires field-aligned propagation of waves. Since the waves were observed at rather high magnetic latitudes, far away from their equatorial source region, they are most probably class I waves which prefer field-aligned direction, see, e.g., *Rauch and Roux* [1982]. Also, the fact that the two wave frequencies correspond well to the field-aligned calculated equatorial He^+ gyrofrequencies supports this assumption.) Alfvén velocity decreases from above 2500 km/s for low-frequency waves to below 1500 km/s for high-frequency waves. Unfortunately, these estimates are undermined by the lack of the other perpendicular electric field component. Furthermore, the magnetic $r2$ component (not shown), which corresponds to the missing electric component, displays somewhat different relative amplitudes for the various bursts than the $r3$ component, implying changes in wave polarization. Therefore, although the overall range of the observed Alfvén velocities is reasonable, the present estimates cannot be taken too rigorously.

However, despite the caveats noted above, it is interesting to study how the difference in local Alfvén velocity between the two wave regions could be explained. Alfvén velocity is proportional to magnetic field density and inversely proportional to the square root of plasma mass density. During the Pc 1 wave observations, Viking was flying to lower latitudes at a slowly decreasing altitude such that magnetic field intensity remained almost constant during this time, decreasing by less than 1%. Thus a change in magnetic field intensity is far too small to explain the observed decrease. However, plasma (mass) density is expected to increase both toward lower latitudes and lower altitudes, and the rate of change can be considerably faster than for the magnetic field. This offers the possibility that the local plasma mass density indeed increased between the two wave sources, leading to the observed decrease in

Alfvén velocity. Thus a decreasing value of Alfvén velocity along the Viking orbit is expected and can be understood in terms of general magnetospheric conditions. Moreover, using the measured magnetic field intensity (about 1650 nT) and the above calculated Alfvén velocity, one can get a rough estimate of the local mass density. Assuming the plasma consists mainly of protons, the number density is about 320 cm^{-3} for Alfvén velocity of 2000 km/s. While this estimate is in the generally correct order of magnitude, it may vary by a factor of 3 around this value for the range of Alfvén velocities mentioned above.

3.4. Burst Durations and Latitudinal Width of Wave Regions

As already discussed above, the Viking electric field instrument observed two intense bursts (B1 and B2) of the low-frequency source and three bursts (B6-B8) of the high-frequency source. The durations of the two low-frequency bursts were roughly similar, about 40 s. However, the high-frequency bursts were slightly shorter, and their duration varied by a factor of 2. The shortest burst (B7) was about 20 s long, and the longest (B6) was about 35 s. (Note also that the amplitude envelope of the low-frequency bursts changed more smoothly than that of the high-frequency bursts.) Nevertheless, the average burst duration observed now is close to that of a sequence of Pc 1 pearls detected by Viking at the same altitude and MLT sector but at somewhat lower latitudes [*Erlandson et al.*, 1992]. As a comparison, it is interesting to note that on the basis of observations from satellites at different altitudes the average duration of EMIC wave bursts seems to increase with altitude from about 5-10 s at a low ionospheric orbit [*Iyemori and Hayashi*, 1989], to 10-25 s above the main ionosphere [*Mursula et al.*, 1994a], and to 30-40 s at the Viking altitude. In a recent statistical survey by DE 2 at an altitude of 300-1000 km, *Erlandson and Anderson* [1996] observed wave durations from a few seconds to above 60 s, with a median of 14 s.

The two low-frequency bursts (B1 and B2) were located at $L = 6.2$ and covered (from start of B1 to end of B2) an L shell range of about 0.18-0.20. This corresponds to an invariant latitude range of about 0.4°-0.5°. Interestingly, nearly the same value (0.5°) is found also for the high-frequency wave region consisting of three bursts (B6-B8). This common estimate for the latitudinal width of the two main EMIC wave regions observed by Viking is in excellent agreement with the earlier result obtained at lower altitudes by the Freja satellite [*Mursula et al.*, 1994a]. There, because of the lower altitude of the Freja satellite only single Pc 1 bursts were observed during a passage through a wave region, and the latitude range was derived from the variation of the burst duration as a function of the geomagnetic inclination of the satellite orbit. Accordingly, the present results give independent and more direct evidence for the previously obtained value and verify the estimate for waves observed at higher altitudes. (We would also like to note that both the previous Freja and the present Viking estimates were obtained during geomagnetically quiet times.) In the present event, more than one burst is observed for both wave regions, and the burst repetition period can be derived for both (see later). If no information about the repetition period exists and only one burst is observed in a wave region, the accuracy of the estimate for the latitude width remains undetermined. This was the case in the earlier low-altitude method [*Mursula et al.*, 1994a], where only statistical arguments could be given in order to exclude the possibility that additional wave bursts might have been missed. Moreover, the burst repetition period observed now is quite short, which makes the latitude width estimate fairly accurate. Accordingly, the present results strongly support the view that the EMIC waves are, at least during geomagnetically quiet times, concentrated to latitudinally fairly narrow shells. (They may, however, be longitudinally much more extended.)

The observed latitudinal width may reflect conditions at the equatorial source region or those during wave propagation from the source toward lower altitudes. The latter may include, for example, density gradients forming suitable ducts for wave propagation [*Mazur and Potapov*, 1983; *Thorne and Horne*, 1992]. Equatorial density enhancements may also exist, which restrict the wave occurrence to the observed narrow latitude width. However, in both models it is quite difficult to explain the two simultaneous Viking sources with similar widths, since a rather fortuitous plasma distribution is needed. Furthermore, the temporal evolution of the high-frequency source would require an appropriate motion of the density enhancement, while the other enhancement of the low-frequency source stays constant for several hours.

Another possibility is that the latitude width is determined by the radial width of the energetic ion population at the equatorial source region of waves. Taking the equatorial magnetic field value of about 130 nT, the Larmor radius of a 100 keV proton is about 0.06 R_e. Thus, the obtained latitude width of about 0.2 L corresponds to only a few equatorial Larmor radii of protons of appropriate energy. Moreover, the equatorial distance between the two wave sources (from $L = 6.2$ to $L = 5.6$) is about ten Larmor radii long. This would suggest that each wave band is produced by a rather localized and coherent group of ions.

3.5. Burst Repetition Period

Let us now study the time differences between the various Viking bursts. We will call the time difference between two subsequent bursts of the same frequency the repetition period of the respective wave source. As we will argue in this section, this is not the repetition period of one and the same wave packet bouncing between the two hemispheres. The repetition period of the low-frequency source (B1-B2) was estimated with

different methods, which gave values varying between 42 s (from burst half widths) to 45 s (from amplitude peak to peak). The repetition time estimated from the lag of the autocorrelation function maximum was 44 s. Accordingly, all these estimates agree within a couple of seconds at $T(\text{low } f) = 43$-44 s. The two repetition periods obtained from the three bursts of the high-frequency source were somewhat different, about 45 s (B6-B7) and 35 s (B7-B8), giving an average repetition period of about 40 s. Moreover, the maximum autocorrelation for bursts B6-B8 was obtained with a lag of about 42 s. Thus the repetition period of the high-frequency source was about $T(\text{high } f) = 40$-42 s, i.e., a few seconds shorter than that of the low-frequency source.

The field line lengths of the low- and high-frequency wave regions are about 15 R_e and 13.5 R_e, respectively. (Very similar values were obtained both from the dipole model and the *Tsyganenko* [1989] model. Note that the late morning MLT sector, moderate invariant latitude, and low geomagnetic activity suggest fairly dipole-like field lines.) If one would assume that the two low-frequency bursts are due to one wave packet bouncing between the two hemispheres along the field line, one obtains, using the above estimate for the burst repetition period, an average propagation velocity of about 4400-4500 km/s. Similarly, the average velocity of the bouncing wave packet producing the high-frequency waves should be about 4200-4400 km/s. (Note that according to the BWP model the Viking bursts should contain both downgoing and upcoming waves which, however, cannot be resolved in the waveform because of the low satellite altitude and high wave speed. Therefore the burst repetition periods derived above correspond to the full length of the field line rather than just the portion above Viking.)

These values are clearly far above any estimates for the propagation speeds of ion cyclotron waves in the magnetosphere. Also, they are considerably higher than the estimates for local Alfvén velocity derived above. The above BWP estimate is the average propagation speed over the whole path, but local velocities vary. Theoretical estimates of the local Alfvén velocity suggest that the velocity decreases at altitudes above Viking but increases at lower altitudes, reaching a maximum at the altitude of a few thousand kilometers and then rapidly decreasing (see, e.g., *Leonovich and Mazur*, 1991; *R.L. Lysak*, Propagation of Alfvén waves through the ionosphere, submitted to the Journal of Geophysical Research, 1997). Accordingly, the local Alfvén velocity measured at Viking gives an upper limit for the Alfvén velocity at altitudes above the spacecraft and a lower limit below it (until the maximum). For a wave packet bouncing back and forth between the two hemispheres the part of the propagation path at altitudes below Viking is only about one third (4 times Viking to ground; about 8-10 R_e) of the whole propagation path. Thus the effective overall velocity below Viking altitude should be correspondingly higher than the Alfvén velocity measured at Viking. However, we noted in section 2.2 that the Viking bursts were observed on ground some 15-20 s later than at Viking. This gives an average propagation speed of about 800-1100 km/s for the path from Viking to ground, i.e., even smaller than the local Alfvén velocity at Viking. This value is also in good agreement with a recent similar estimate by *Erlandson et al.* [1996], who derived the Pc 1 wave transit time from Viking to ground to be 12 ± 2 s (corresponding to average propagation speed of 1000-1100 km/s) at a similar altitude and only slightly lower L. Assuming the effective propagation speed at altitudes below Viking to be about 1100 km/s implies that the wave spends at least 48 s at these low altitudes, i.e., longer than the observed burst repetition period, leaving no time for propagation at altitudes above Viking. This result is a clear contradiction with the BWP hypothesis. Moreover, as noted above, the Alfvén velocity is expected to decrease above Viking. Using the measured Alfvén velocity of the Viking low-frequency source implies that the wave spends at least 45-50 s at altitudes above Viking. Note also that the heavy ion effects (nonzero frequency effects) tend to decrease the wave group velocity close to the equator where wave frequency approaches the local heavy ion gyrofrequency [*Fraser*, 1972; *Ludlow and Hughes*, 1993]. It has been estimated [*Erlandson et al.*, 1992] that this effect decreases the overall propagation speed to approximately one half of the Alfvén velocity. Accordingly, the nonzero frequency effect will further strengthen the disagreement with the BWP hypothesis.

However, one might think that the two bursts of the low-frequency source might be due to one packet that is first going down and soon coming up. Using the path length of 4-5 R_e and the above time difference, one finds an average speed of about 600-750 km/s, which is quite a reasonable estimate [*Erlandson et al.*, 1996; *Erlandson and Anderson*, 1996]. However, there are several arguments which deny this possibility. First, according to this scenario the upcoming burst should be clearly weaker than the downgoing wave. The fraction of reflected (upcoming) wave flux has been limited quite small, below 10-20%, by *Erlandson et al.* [1992]. However, our observations show that the second burst is at least as strong as the first one. Second, we calculated the field-aligned component of the Poynting flux and found no significant difference between the two bursts. Both bursts included both upward and downward parts with the latter dominating. Third, the same idea does not apply to the three bursts of the high-frequency source, because either of the two time differences should correspond to the (nearly) full path to and from the other hemisphere, leading to the above discussed difficulty. The longer time gap between B6 and B7 of course would suggest that B6 and B8 are upcoming and B7 is downgoing. Taking into account that B7 is weaker than the two other bursts, this leads to the same problem with amplitudes as in case of the low-

frequency bursts. Also, the Poynting flux of the three high-frequency bursts was even more clearly downward dominated than for the low-frequency bursts. Therefore we are convinced that the bouncing wave packet hypothesis cannot be reconciled with the present observations in any possible configuration of the wave bursts.

3.6. Alternate Models of Burst Generation

Two alternatives to the bouncing wave packet hypothesis, which both include an equatorial modulator of Pc 1 waves, were discussed recently by *Erlandson et al.* [1992]. One mechanism is based on the observation that the bounce period of ions with energies suitable for Pc 1 production are close to the observed wave repetition period. For example, the appropriate proton energy corresponding to the observed wave repetition period ranges from about 35 keV to about 120 keV, depending on the pitch angle varied here from 85° to 5°. (The energy required from heavier ions would be correspondingly higher.) Accordingly, phase-bunched ions bouncing from one hemisphere to another would produce one wave packet at every equatorial crossing. The wave repetition period on the ground would, however, be the same as the ion bounce period, since the resonance condition requires an antiparallel motion of ions and waves. Thus only every second crossing would produce a wave packet propagating in the same direction. However, the main problem for this model is to develop a detailed physical theory for the phase bunching of ions. Moreover, observational evidence for this mechanism is still quite meager.

Another alternative model for producing nonbouncing Pc 1 wave bursts invokes long-period ULF waves. This model is based on the idea that a ULF wave that has a sufficiently large amplitude at the equatorial Pc 1 source region could affect the relevant plasma parameters and thus modify the Pc 1 growth rate. This would lead to Pc 1 wave generation whose amplitude varies at the period of the long-period wave. For example, variations of magnetic field intensity induced by a compressional ULF wave could cause a change in Pc 1 growth rate by increasing the ion temperature anisotropy above the critical value [*Cornwall,* 1966; *Kennel and Petschek,* 1966; *Olson and Lee,* 1983]. In order to have large variations in Pc 1 wave growth (and little growth at a certain phase) this model requires that plasma is close to the conditions leading to ion cyclotron instability. EMIC wave generation in such marginally stable conditions was studied recently [*Gail,* 1990].

Erlandson et al. [1992] did not observe long-period waves during their pearl Pc 1 event, making them conclude that if the ULF wave model should work at all, the long-period waves should be localized around the equator. Such localized waves have indeed been found [*Engebretson et al.,* 1988]. However, they were found to be mainly radially polarized with little power in the compressional component, excluding a straightforward identification with the proposed mechanism. In a recent paper, *Plyasova-Bakounina et al.* [1996] studied events where simultaneous Pc 1 and Pc 4/5 pulsations were observed on the ground and Pc 1 bursts were repeated at Pc 4/5 oscillation period. Similar observations have also been made close to the equator by the CRRES satellite [*Rasinkangas et al.,* 1994]. In the present event, strong Pc 3/4 waves were observed on the ground at all stations with a period close to 40 s. Therefore the ULF wave model seems to be supported in the present case. These observations are currently being analyzed, and the results will be published in another paper.

Finally, we would like to note that the ratio of the field line length and the observed repetition period was found to be almost the same for the two wave sources. In the phase-bunching model this is trivially explained. However, the ULF wave model may accommodate this fact as well. It is well known, for example, that in the case of a field line resonance the ULF wave period changes with latitude. If the plasma density remains constant with latitude (or changes slowly within the limited latitude range), the period is essentially proportional to the field line length, in agreement with present observations.

4. Summary and Conclusion

In this paper we have analyzed a Pc 1 event where initially one wave band on the ground was observed to evolve smoothly to two separate bands. This separation was verified in space by the Viking satellite, which passed through the two wave regions in the middle of the event. The outer (inner) wave region at $L = 6.2$ ($L = 5.6$) had a frequency of about 0.3 Hz (0.5 Hz), both below the calculated equatorial helium gyrofrequency. The higher frequency at lower latitude is in agreement with the corresponding increase of the equatorial magnetic field intensity.

We estimated the Alfvén velocity from the ratio of one transverse electric component and the corresponding magnetic wave component. The low-frequency waves had a somewhat larger Alfvén velocity (about 2500 km/s) than the high-frequency waves (1000-1500 km/s). (However, this estimate suffers from the lack of the other transverse electric field component.) In both source regions the waves were constrained to a narrow latitude range of about 0.5° of invariant latitude, in accordance with similar estimates from satellite observations at lower altitudes [*Mursula et al.,* 1994a].

Both of the two Viking wave source regions consisted of separate, repeated wave bursts. The burst duration was about 30-40 s, well in agreement with earlier observations during a Pc 1 pearl event at similar altitudes [*Erlandson et al.,* 1992] and somewhat longer than observed at lower altitudes [*Iyemori and Hayashi,* 1989; *Mursula et al.,* 1994a]. The burst repetition periods were roughly the same for both wave regions, about 40-45 s, and somewhat shorter than observed earlier during a pearl Pc 1 event at a fairly similar spatial location [*Er-*

landson et al., 1992]. After a detailed analysis of the repeated bursts we conclude that the observed wave bursts cannot be produced by a wave packet bouncing between the two hemispheres, a hypothesis which has been the paradigm for repetitive Pc 1 emissions observed on the ground for more than 30 years [*Jacobs and Watanabe,* 1964; *Obayashi,* 1965].

We discussed two alternatives to the bouncing wave packet model. One model invokes phase-bunched energetic ions, and the other invokes long-period ULF waves. According to both models, Pc 1 wave growth is modulated at or close to the equatorial source regions of waves, where separate wave bursts are formed. The wave bursts propagate from the equatorial source region into the two ionospheres, explaining naturally the fact that the Poynting flux is directed away from the equator [*Mauk and McPherron,* 1980; *Erlandson et al.,* 1990; *LaBelle and Treumann,* 1992; *Fraser et al.,* 1996]. We noted that in the present event, strong Pc 3/4 waves are observed on the ground with a period coinciding well with the repetition period of the observed Pc 1 bursts. These ULF waves will be analyzed in more detail in a subsequent publication.

We note that the ground waves of the present event were classified as hydromagnetic chorus type Pc 1's [*Fukunishi et al.,* 1981] rather than pearl Pc 1's because of a strong diffuse background. However, the wave intensity on the ground was strongly fluctuating, and several dispersive pearls were observed among the diffuse background. It is evident from the presented Viking results that the HM chorus events may consist of similar repetitive bursts as observed for pearl waves. We found that most properties (frequency, amplitude, burst duration, latitude width) of the bursts of the present HM event were the same as those of a pearl wave [*Erlandson et al.,* 1992]. This suggests a close connection between the pearl and HM chorus type Pc 1's.

The burst repetition period was somewhat shorter in the present HM event than found earlier for a pearl event at similar altitude and MLT sector but with a lower L shell [*Erlandson et al.,* 1992]. (In fact, the higher repetition rate of HM bursts may be the reason why these waves have a large diffuse background and are classified as HM chorus. If there is more than one wave source with slightly different repetition periods, the bursts could interfere on the ground and lead to a diffuse signal with no clear repetitive structure. This would occur more easily in case of high than low repetition rate.) The possibility that the higher-latitude HM bursts might, generally, have a shorter repetition period than the similar pearl bursts at lower latitudes is very important, since it can be used to distinguish between the two models discussed above as alternatives to the bouncing wave packet model. The model of phase-bunched ions predicts a continuous increase of the repetition period with latitude (field line length), thus contradicting with the above scenario. However, the ULF model can explain the observations by the effect of the plasma density on wave period. Considerably longer (shorter) wave periods for the same wave mode are predicted inside (outside) the plasmapause on rather close-by field lines. Since pearls are known to occur mainly inside the plasmapause [*Taylor and Lyons,* 1976; *Fraser et al.,* 1989; *Erlandson et al.,* 1990, 1992, 1996], their observed longer repetition period can be understood by the ULF model. The shorter repetition period of the HM bursts agrees with the fact that they occur at higher latitudes, outside the plasmapause.

In the present case, spacecraft potential measurements indicate a constant slow increase of plasma density before, during, and somewhat after the event. Although no clear signal for plasmapause was observed (most probably because of observational constraints), the relative rate of change and absolute level of potential suggest that plasmapause was located at about $L = 5.2$. Also, the plasmapause model by *Carpenter and Anderson* [1992], when calculated for conditions prevailing during the present event, locates both Viking Pc 1 sources close to the outer edge of the plasmapause, in agreement with the ULF model.

Concluding, we note that the results presented in this paper form a new and unifying scenario between different Pc 1 wave types, in particular, the pearl Pc 1's and HM chorus. While the pearls are modulated Pc 1 waves propagating within or at the plasmapause, the HM chorus events consist of similar wave packets propagating outside the plasmasphere. Moreover, since the bouncing wave packet model could be excluded in the present paper as an explanation for the exoplasmaspheric Pc 1 (IIM chorus) bursts, it is natural to suggest that the same is true for more clear (plasmaspheric) pearl events as well. The above results suggest that Pc 1 modulation by ULF waves is the more viable candidate out of the two alternative models discussed.

Acknowledgments. We thank J. Kangas for discussions, R. Kuula for efficient help in data retrieval and programming, and L. Kalliopuska for layout production. We acknowledge the two referees for useful comments and suggestions. Finally, the Academy of Finland is acknowledged for financial support.

The editor thanks Richard M. Thorne and W. Jeffrey Hughes for their assistance in evaluating this paper.

References

Anderson, B. J., R. E. Erlandson, and L. Zanetti, A statistical study of Pc 1-2 magnetic pulsations in the equatorial magnetosphere, 1, Equatorial occurrence distributions, *J. Geophys. Res., 97,* 3075-3088, 1992a.

Anderson, B. J., R. E. Erlandson, and L. J. Zanetti, A statistical study of Pc 1-2 magnetic pulsations in the equatorial magnetosphere, 2, Wave properties, *J. Geophys. Res., 97,* 3089-3101, 1992b.

Benioff, H., Observations of geomagnetic fluctuations in the period range 0.3 to 120 seconds, *J. Geophys. Res., 65,* 1413-1422, 1960.

Bossen, M., R. L. McPherron, and C. T. Russell, A statistical study of Pc 1 magnetic pulsations at synchronous orbit, *J. Geophys. Res., 81,* 6083-6091, 1976.

Brice, N., Generation of very low frequency and hydromagnetic emissions, *Nature, 206,* 283-284, 1965.

Carpenter, D. L., and R. R. Anderson, An ISEE/Whistler model of equatorial electron density in the magnetosphere, *J. Geophys. Res., 97,* 1097-1108, 1992.

Cornwall, J. M., Cyclotron instabilities and electromagnetic emission in the ultra low frequency and very low frequency ranges, *J. Geophys. Res., 70,* 61-69, 1965.

Cornwall, J. M., Micropulsations and the outer radiation zone, *J. Geophys. Res., 71,* 2185-2199, 1966.

Criswell, D., Pc 1 micropulsation activity and magnetospheric amplification of 0.2- to 5.0-Hz hydromagnetic waves, *J. Geophys. Res., 74,* 205-224, 1969.

Engebretson, M. J. , L. J. Zanetti, T. A. Potemra, D. M. Klumpar, R. J. Strangeway, and M. H. Acuna, Observations of intense ULF pulsation activity near the geomagnetic equator during quiet times, *J. Geophys. Res., 93,* 12795-12816, 1988.

Erlandson, R. E., and B. J. Anderson, Pc 1 waves in the ionosphere: A statistical study, *J. Geophys. Res. 101,* 7843-7857, 1996.

Erlandson, R. E., L. J. Zanetti, T. A. Potemra, L. P. Block, and G. Holmgren, Viking magnetic and electric field observations of Pc 1 waves at high latitudes, *J. Geophys. Res., 95,* 5941-5955, 1990.

Erlandson, R. E., B. J. Anderson, and L. J. Zanetti, Viking magnetic and electric field observations of periodic Pc 1 waves: Pearl pulsations, *J. Geophys. Res., 97,* 14823-14832, 1992.

Erlandson, R. E., K. Mursula, and T. Bösinger, Simultaneous ground-satellite observations of structured Pc 1 pulsations, *J. Geophys. Res., 101,* 27149-27156, 1996.

Fraser, B. J., Propagation of Pc 1 micropulsations in a proton-helium magnetosphere, *Planet. Space Sci., 20,* 1883-1893, 1972.

Fraser, B. J., W. J. Kemp, and D. J. Webster, Ground-satellite study of a Pc 1 ion cyclotron wave event, *J. Geophys. Res., 94,* 11855-11863, 1989.

Fraser, B. J., H. J. Singer, W. J. Hughes, J. R. Wygant, R. R. Anderson, and Y. D. Hu, CRRES Poynting vector observations of electromagnetic ion cyclotron waves near the plasmapause, *J. Geophys. Res., 101,* 15331-15343, 1996.

Fukunishi, H., T. Toya, K. Koike, M. Kuwashima, and M. Kawamura, Classification of hydromagnetic emissions based on frequency-time spectra, *J. Geophys. Res., 86,* 9029-9039, 1981.

Gail, W. B., Theory of electromagnetic cyclotron wave growth in a time-varying magnetoplasma, *J. Geophys. Res., 95,* 19089-19097, 1990.

Gendrin, R., S. Lacourly, A. Roux, J. Solomon, F. Z. Feygin, M. V. Gokhberg, V. A. Troitskaya, and V. L. Yakimenko, Wave packet propagation in an amplifying medium and its application to the dispersion characteristics and to the generation mechanism of Pc 1 events, *Planet. Space Sci., 19,* 165-194, 1971.

Gendrin, R., S. Perraut, H. Fargetton, F. Glangeaud, and J. Lacoume, ULF waves: Conjugated ground-satellite relationships, *Space Sci. Rev., 22,* 433-442, 1978.

Gomberoff, L., and R. Neira, Convective growth rate of ion cyclotron waves in a H^+-He^+ and H^+-He^+-O^+ plasma, *J. Geophys. Res., 88,* 2170-2174, 1983.

Harang, L., Oscillations and vibrations in magnetic records at high-latitude stations, *J. Geophys. Res., 41,* 329-336, 1936.

Horne, R. B., and R. M. Thorne, Convective instabilities of electromagnetic ion cyclotron waves in the outer magnetosphere. *J. Geophys. Res. 99,* 17259-17273, 1994.

Hultqvist, B., The Viking project, *Geophys. Res. Lett., 14,* 379-382, 1987.

Iyemori, T., and K. Hayashi, Pc 1 micropulsations observed by Magsat in the ionospheric *F* region, *J. Geophys. Res., 94,* 93-100, 1989.

Jacobs, J. A., and T. Watanabe, Micropulsation whistlers, *J. Atmos. Terr. Phys., 26,* 825-829, 1964.

Kaye, S. M., and M. G. Kivelson, Observations of Pc 1-2 waves in outer magnetosphere, *J. Geophys. Res., 84,* 4267-4276, 1979.

Kennel, C. F., and H. E. Petschek, Limit on stably trapped particle fluxes, *J. Geophys. Res., 71,* 1-28, 1966.

Kozyra, J. U., T. E. Cravens, A. F. Nagy, E. G. Fontheim, and R. S. B. Ong, Effects of energetic heavy ions on electromagnetic ion cyclotron wave generation in the plasmapause region, *J. Geophys. Res., 89,* 2217-2233, 1984.

LaBelle, J., and R. A. Treumann, Poynting vector measurements of electromagnetic ion cyclotron waves in the plasmasphere, *J. Geophys. Res., 97,* 13789-13979, 1992.

Leonovich, A. S., and V. A. Mazur, An electromagnetic field, induced in the ionosphere and atmosphere and on the Earth's surface by low-frequency Alfvén oscillations of the magnetosphere: General theory, *Planet. Space Sci., 39,* 529-546, 1991.

Lewis, P. B., Jr., R. L. Arnoldy, and L. J. Cahill Jr., The relation of Pc 1 micropulsations measured at Siple, Antarctica, to the plasmapause, *J. Geophys. Res., 82,* 3261-3271, 1977.

Ludlow, G. R., and W. J. Hughes, The ion cyclotron group delay for source regions near the plasmapause, *J. Geophys. Res., 98,* 7561-7570, 1993.

Mauk, B. H., and R. L. McPherron, An experimental test of the electromagnetic ion cyclotron instability within the Earth's magnetosphere, *Phys. Fluids, 23,* 2111-2126, 1980.

Mazur, V. A, and A. S. Potapov, The evolution of pearls in the Earths magnetosphere, *Planet. Space Sci., 31,* 859-863, 1983.

McPherron, R. L., C. T. Russell, and P. J. Coleman Jr., Fluctuating magnetic fields in the magnetosphere, 2, ULF waves, *Space Sci. Rev., 13,* 411-454, 1972.

Mursula, K., L. G. Blomberg, P. A. Lindqvist, G. T. Marklund, T. Bräysy, R. Rasinkangas, and P. Tanskanen, Dispersive Pc 1 bursts observed by Freja, *Geophys. Res. Lett., 21,* 1851-1854, 1994a.

Mursula, K., J. Kangas, and T. Pikkarainen, Properties of structured and unstructured Pc 1 pulsations at high latitudes: Variation over the 21st solar cycle, in *Solar Wind Sources of Magnetospheric Ultra-Low-Frequency Waves, Geophys. Monogr., Ser., vol. 81,* edited by M. J. Engebretson, K. Takahashi, and M. Scholer, pp. 409-415, AGU, Washington, D. C., 1994b.

Mursula, K., B. J. Anderson, R. E. Erlandson, and T. Pikkarainen, Solar cycle change of Pc 1 waves observed by an equatorial satellite and on the ground, *Adv. Space Res., 17(10),* 51-55, 1996.

Obayashi, T., Hydromagnetic whistlers, *J. Geophys. Res., 70,* 1069-1087, 1965.

Olson, J. V., and L. C. Lee, Pc 1 wave generation by sudden impulses, *Planet. Space Sci., 31,* 295-302, 1983.

Plyasova-Bakounina, T. A., J. Kangas, K. Mursula, O. A. Molchanov, and J. A. Green, Pc 1-2 and Pc 4-5 pulsations observed at a network of high-latitude stations, *J. Geophys. Res. 101,* 10965-10973, 1996.

Rasinkangas, R., K. Mursula, G. Kremser, H. J. Singer, B. J. Fraser, A. Korth, and W. J. Hughes, Simultaneous occurrence of Pc 5 and Pc 1 pulsations in the dawnside magnetosphere: CRRES observations, in *Solar Wind Sources of Magnetospheric Ultra-Low-Frequency Waves, Geophys. Monogr., Ser., vol. 81,* edited by M. J. Engebretson, K. Takahashi, and M. Scholer, pp. 417-424, AGU, Washington, D. C., 1994.

Rauch, J. L., and A. Roux, Ray-tracing of ULF waves in a multicomponent magnetospheric plasma: Consequences for the generation mechanism of ion cyclotron waves, *J. Geophys. Res., 87,* 8191-8198, 1982.

Roth, B., and D. Orr, Locating the Pc 1 generation region by a statistical analysis of ground-based observations, *Planet. Space Sci., 23,* 993-1002, 1975.

Roux, A., S. Perraut, J. L. Rauch, C. de Villedary, G. Kremser G., A. Korth, and D. T. Young, Wave-particle interactions near Ω_{He^+} observed on GEOS 1 and 2, 2, Generation of ion cyclotron waves and heating of He^+ ions, *J. Geophys. Res., 87,* 8174-8190, 1982.

Saito, T., Geomagnetic pulsations, *Space Sci. Rev., 10,* 319-412, 1969.

Sucksdorff, E., Occurrence of rapid micropulsations at Sodankyl during 1932 to 1935, *J. Geophys. Res., 41,* 337-344, 1936.

Taylor, W. W. L., and L. R. Lyons, Simultaneous equatorial observations of 1- to 30-Hz waves and pitch angle distributions of ring current ions, *J. Geophys. Res., 81,* 6177-6183, 1976.

Thorne, R. M., and R. B. Horne, The contribution of ion-cyclotron waves to electron heating and SAR-arc excitation near the storm-time plasmapause, *Geophys. Res. Lett., 19,* 417-420, 1992.

Troitskaya, V. A., and A. V. Guglielmi, Geomagnetic micropulsations and diagnostics of the magnetosphere, *Space Sci. Rev., 7,* 689-768, 1967.

Troitskaya, V. A., and A. V. Guglielmi, Hydromagnetic diagnostics of plasma in the magnetosphere, *Ann. Geophys. 26,* 893-902, 1970.

Tsyganenko, N. A., A magnetospheric magnetic field model with a warped tail current sheet, *Planet. Space Sci, 37,* 5-20, 1989.

Webster, D. J., and B. J. Fraser, Source regions of low-latitude Pc 1 pulsations and their relationship to the plasmapause, *Planet. Space Sci., 33,* 777-793, 1985.

Young, D. T., S. Perraut, A. Roux, C. De Villedary, R. Gendrin, A. Korth, G. Kremser, and D. Jones, Wave-particle interactions near Ω_{He^+} observed on GEOS 1 and 2, 1, Propagation of ion cyclotron waves in He^+-rich plasma, *J. Geophys. Res., 86,* 6755-6772, 1981.

K. Mursula, R. Rasinkangas, and T. Bösinger, Department of Physical Sciences, University of Oulu, P.O.Box 333, FIN-90571 Oulu, Finland

R. E. Erlandson, Applied Physics Laboratory, Johns Hopkins University, Laurel, MD 20723-6099.

P.-A. Lindqvist, Royal Institute of Technology, Alfvén Laboratory, S-10044 Stockholm, Sweden

(Received November 5, 1996; revised March 25, 1997; accepted April 1, 1997.)